Biomaterials 62 (2015) 1–12

Contents lists available at ScienceDirect

Biomaterials

journal homepage: www.elsevier.com/locate/biomaterials

The *microwell-mesh*: A novel device and protocol for the high throughput manufacturing of cartilage microtissues

Kathryn Futrega [a, 1], James S. Palmer [a, 1], Mackenzie Kinney [a, 1], William B. Lott [a, b, 1], Mark D. Ungrin [c, 2], Peter W. Zandstra [d, 3], Michael R. Doran [a, e, *]

[a] Institute of Health and Biomedical Innovation, Queensland University of Technology at The Translational Research Institute, Brisbane, QLD, Australia
[b] School of Chemistry, Physics and Mechanical Engineering, Science and Engineering Faculty, Queensland University of Technology Brisbane, QLD, Australia
[c] Department of Comparative Biology and Experimental Medicine, Faculty of Veterinary Medicine, University of Calgary, Alberta, Canada
[d] Institute of Biomaterials and Biomedical Engineering, University of Toronto, Ontario, Canada
[e] Mater Medical Research – University of Queensland, Brisbane, QLD, Australia

ARTICLE INFO

Article history:
Received 6 February 2015
Received in revised form
4 May 2015
Accepted 14 May 2015
Available online 20 May 2015

Keywords:
Microwell
Microtissue
3D culture
Stem cell
Cartilage
Mesenchymal stromal cell
Chondrocyte
Differentiation

ABSTRACT

Microwell platforms are frequently described for the efficient and uniform manufacture of 3-dimensional (3D) multicellular microtissues. Multiple partial or complete medium exchanges can displace microtissues from discrete microwells, and this can result in either the loss of microtissues from culture, or microtissue amalgamation when displaced microtissues fall into common microwells. Herein we describe the first microwell platform that incorporates a mesh to retain microtissues within discrete microwells; the ***microwell-mesh***. We show that bonding a nylon mesh with an appropriate pore size over the microwell openings allows single cells to pass through the mesh into the microwells during the seeding process, but subsequently retains assembled microtissues within discrete microwells. To demonstrate the utility of this platform, we used the microwell-mesh to manufacture hundreds of cartilage microtissues, each formed from 5×10^3 bone marrow-derived mesenchymal stem/stromal cells (MSC). The microwell-mesh enabled reliable microtissue retention over 21-day cultures that included multiple full medium exchanges. Cartilage-like matrix formation was more rapid and homogeneous in microtissues than in conventional large diameter control cartilage pellets formed from 2×10^5 MSC each. The microwell-mesh platform offers an elegant mechanism to retain microtissues in microwells, and we believe that this improvement will make this platform useful in 3D culture protocols that require multiple medium exchanges, such as those that mimic specific developmental processes or complex sequential drug exposures.

1. Introduction

Cell behavior in 3-dimensional (3D) *in vitro* cultures can fundamentally differ from that in 2D cultures [1]. Cells in 3D cultures experience fewer physical restrictions, allowing them to more readily establish microenvironments with enhanced cell–cell communication, organization and production of extracellular matrix (ECM) [2]. The common approaches used to generate 3D tissues *in vitro* have been recently reviewed [3], and each has its own appeal depending on the application. An increasingly favored 3D culture approach in cancer cell biology, organoid culture and cartilage tissue engineering is the formation of multicellular aggregates, termed microtissues [1–5]. Microtissues have been manufactured for decades by aggregating hundreds-to-thousands

* Corresponding author. Queensland University of Technology at the Translational Research Institute, 37 Kent Street, Brisbane, QLD 4102, Australia.
E-mail addresses: k.futrega@qut.edu.au (K. Futrega), james.palmer@qut.edu.au (J.S. Palmer), mackenziekinney@gmail.com (M. Kinney), b.lott@qut.edu.au (W.B. Lott), mdungrin@ucalgary.ca (M.D. Ungrin), peter.zandstra@utoronto.ca (P.W. Zandstra), michael.doran@qut.edu.au (M.R. Doran).
[1] Queensland University of Technology at the Translational Research Institute, 37 Kent Street, Brisbane, QLD 4102, Australia.
[2] Department of Comparative Biology and Experimental Medicine, Faculty of Veterinary Medicine, University of Calgary, HMRB 320, 3330 Hospital Drive NW, Calgary, Alberta T2N 4N1, Canada.
[3] The Donnelly Centre for Cellular and Biomolecular Research, University of Toronto, 160 College Street, Room 1116, Toronto, Ontario M5S 3E1, Canada.

http://dx.doi.org/10.1016/j.biomaterials.2015.05.013

of cells in either a single droplet (hanging drop) or in non-adherent tissue culture vessels [1]. While often favored over conventional 2D cultures, these relatively labor-intensive methodologies have delayed the widespread adoption of 3D microtissue culture [1,3]. Recent technological advances and the commercial availability of products that enable high throughput microtissue manufacture via microfluidic-based hanging drop, micro-patterned surfaces or microwell platforms are increasingly bringing 3D microtissue culture into mainstream practice [3].

Microtissues are appealing building blocks in tissue engineering applications [3,4,6–8], including the manufacture of cartilage microtissues from either mesenchymal stem/stromal cells (MSC) [5] or articular chondrocytes [8]. The fundamental motivation for using a microwell platform to manufacture cartilage microtissues is its capacity to reproducibly generate hundreds of uniform microtissue building blocks. This is achieved either through forced aggregation (centrifugation) or gravity settling of a cell suspension into an array of microwells placed at the bottom of a larger tissue culture well [9]. Once the cells have settled into discrete microwells they generally amalgamate within a few hours, and then mature into uniform cartilage microtissues over the subsequent culture period [5,8]. Complete medium exchange is often required to feed microtissues, to sequentially modify the exogenous signal microenvironment, and/or to guide the appropriate development of artificial cartilage tissue. Complete or even partial medium exchange can generate turbulence that is sufficient to dislodge microtissues from their individual microwells. While careful manipulation can reduce the frequency of microtissue displacement from microwells, cartilage microtissues have a propensity to adhere to each other making them particularly challenging to culture using conventional microwell systems. This challenge is exasperated when cultures are scaled into larger 6-well formats or when multiple full medium exchanges are required. Dislodged microtissues that accumulate in individual microwells tend to merge into single tissues of uncontrolled size and geometry. This variability diminishes the advantages of microwell systems, and hampers the development of complex medium exchange protocols. Such protocols are likely required to generate hyaline cartilage from MSC [11] or to manufacture cartilage microtissues on a large-scale for clinical applications.

To address the above problems in cartilage microtissue manufacture, and to more generally improve upon the current microwell platforms, we have developed a microwell platform with a nylon mesh fixed over the microwell openings, which we term the "*microwell-mesh*". The pores in the mesh are sufficiently large to permit single cells to pass into the microwells. Once the cells aggregate within the microwell, the resulting microtissue is too large to pass back out through the mesh and remains trapped within its discrete microwell. Herein we outline the microwell-mesh fabrication methodology, and describe the application of the microwell-mesh innovation to high throughput cartilage microtissue manufacture. Specifically, we contrast the differentiation and cartilage-like matrix formation of bone marrow-derived MSC either aggregated into singular pellets of 2×10^5 MSC each (control pellet cultures) or into hundreds of microtissues of approximately 5×10^3 MSC each (cartilage microtissues) using the microwell-mesh platform.

2. Methods

2.1. Microwell mold manufacture

The microwell surfaces were produced using a reverse templating process. An acrylic sheet with a pyramidal array was purchased from Mulford Plastics (Australia), and served as the initial mold. Each pyramidal well on the acrylic sheet was 2 mm × 2 mm square, by 0.8 mm deep. A negative impression was created by casting a 10 mm thick layer of polydimethylsiloxane (PDMS, Sylgard184; Dow Corning, Midland MI, USA) over the acrylic surface. The PDMS was allowed to cure for 1 h at 80 °C and then removed from the acrylic mold and incubated at 80 °C for an additional 72 h. Incorporation of the additional curing time crystalizes the PDMS surface sufficiently to prevent bonding during the double casting of PDMS [12]. The PDMS negative impression was then used to generate a 10 mm thick PDMS positive impression of the original acrylic surface. The positive PDMS impression layer was cured for 60 min at 80 °C, and then peeled from the PDMS negative impression. Finally, a reusable negative template surface was formed using a hot press (POWER TEAM hydraulic heat press) at 160 °C for 15 min to press the final PDMS surface template into sheets of polystyrene. Polystyrene sheets were cut from 500 cm^2 cell culture dishes (Corning, NY USA). The hot pressed polystyrene negatives were then used to generate sheets of PDMS having the microwell surface pattern.

2.2. Microwell and microwell-mesh fabrication

Microwell-mesh fabrication is summarized schematically in Fig. 1A. In brief, a 3 mm deep layer of PDMS was poured on the polystyrene negative template and cured for 60 min at 80 °C. Discs were punched from the PDMS sheet using a 35 mm diameter Priory wad punch (Amazon.com), producing discs that fit snugly into 6-well plates. Square pieces (4 cm × 4 cm) cut out from a sheet of nylon (6/6) mesh (36 μm square pore openings, part number: CMN-0035, Amazon.com) were bonded to the open face of the microwell discs using silicone glue (Selleys Aquarium Safe, Padstow, New South Wales). To apply a thin layer of silicone glue over the microwells, a foam biopsy pad (Fisherbrand) was saturated with silicone glue and excess glue dabbed off onto a waste surface prior to gently dabbing the top of the microwell discs. The square of nylon mesh was applied over top and pressed down to ensure adequate contact with the top edges of the PDMS microwells. The silicone glue fixing the nylon mesh was cured overnight at room temperature, and the excess mesh was then trimmed from the edge of the microwell disc. A small dab of silicone glue was used to anchor the microwell disc insert in a well of a 6-well plate (Cat#: CLS3516, Corning). The silicone glue anchoring the microwell disc inserts was cured for 60 min on an 80 °C hot plate. PDMS was selected for the manufacture of the base microwell platform as PDMS rapid fabrication is inexpensive, versatile, and has been successfully used to manufacture microwells in similar studies [4,8]. Nylon (6/6) was selected for use in the mesh as nylon is a non-toxic biocompatible material commonly used in clinical applications including formation of gastrointestinal segments, vascular grafts, and sutures [13]. Critically, nylon (6/6) meshes with tailored pore sizes can be readily purchased from commercial vendors.

2.3. Microwell-mesh characterization via micro-computed tomography (mCT)

Micro–computed tomography (mCT) was used to characterise the shape and dimension of the cavities in the microwell-mesh. To enhance the contrast, the microwell-mesh fibers and surface were sputter coated with gold (Leica EM SCD005 sputter coater). All mCT workflows were performed on the mCT subsystem of an Inveon Multimodality PET-mCT (Siemens, Munich Germany) system equipped with a variable focal spot X-ray source. 720 projection images were acquired in a 360° rotation around the sample, with a field of view of 1024 × 1152 pixels. The imaging protocol for the standard detector used X-ray settings of 80 kVp at 0.5 mA with a

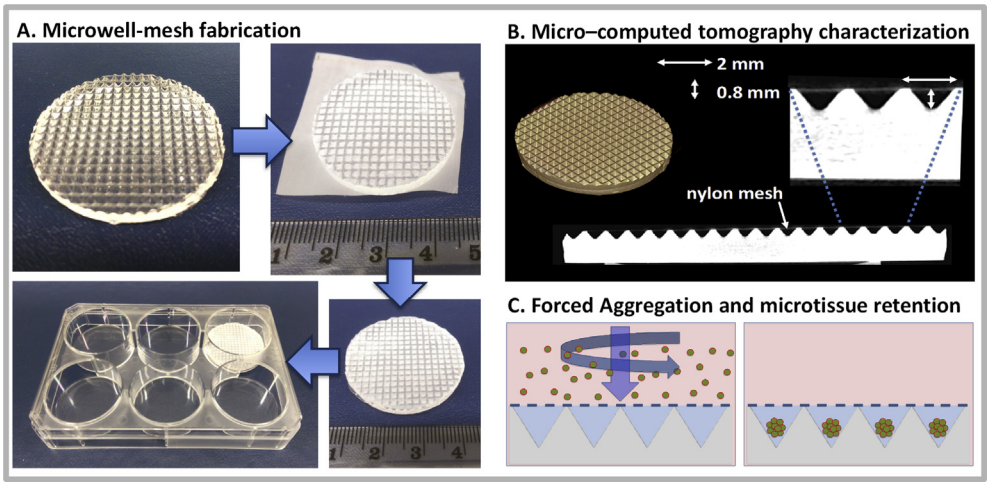

Fig. 1. (A) Fabrication of microwell-mesh inserts. PDMS sheets with microwells 2 mm × 2 mm square, by 0.8 mm deep were cast on a polystyrene mold. Discs 35 mm in diameter were punched from the sheets. Nylon mesh was bonded to the top of the microwell disc creating the microwell-mesh system. The nylon mesh was then trimmed to align with the edge of the PDMS disc, and the discs were anchored in 6-well plates using silicone glue. (B) Micro-computed tomography of the microwell-mesh shows the shape and dimensions of the microwells. Microwells were confirmed to be 2 mm × 2 mm × 0.8 mm deep. The nylon mesh was bonded to the top of each microwell forming sealed discreet culture microwells. (C) Cells were pelleted through the nylon mesh into microwells via forced aggregation. Cells that had amalgamated into microtissues were too large to pass back through the nylon mesh and were retained in discreet microwells.

0.5 mm aluminium filter and a 1000 ms exposure time. The images were acquired with a bin factor of 2 and were reconstructed using the Feldkamp algorithm with no down sampling, resulting in images with pixels of 36 μm in each dimension. All image processing and analysis was performed on the Inveon Research Workplace 4.2 software package.

2.4. Microwell-mesh sterilization

The microwell-mesh inserts were sterilized with 70% ethanol/water. To ensure that all surfaces contacted the sterilizing solution, 4 mL of 70% ethanol was aliquoted into each well and then the plate was centrifuged at 2000 × g for 2 min. The plate was then entirely submerged in 70% ethanol and incubated for 60 min at room temperature. Following incubation in ethanol, the wells were washed twice with 4 mL of PBS (Life Technologies, Mulgrave, Australia). During the second rinse the plates were again centrifuged at 2000 × *g* for 2 min to ensure that the PBS had displaced the ethanol. The wells were rinsed a third time with 4 mL of PBS and left to soak overnight to elute any residual ethanol from the PDMS. If the plates were to be stored for future use, sterile water was used instead of PBS and the plates were dried. Immediately prior to use, the microwell-mesh inserts were washed with a sterile solution of 5% Pluronic (F-127 Pluronic, Sigma Aldrich, Castle Hill, Australia) in PBS. Pluronic adsorbs onto the PDMS surface, rendering it non-adhesive and thereby promoting cell aggregation [4,9]. The plate was centrifuged at 2000 × g for 2 min to ensure that the Pluronic solution contacted all surfaces and that any bubbles were displaced from the microwells. The Pluronic was permitted to adsorb for at least 5 min before rinsing with 4 mL of PBS.

2.5. Mesenchymal stem/stromal cell (MSC) isolation and culture

MSC isolation and characterization was performed similarly to previously described [5]. Bone marrow aspirates (BMA) were collected from the iliac crest of fully informed and consenting healthy volunteer donors. The Mater Health Services Human Research Ethics Committee and the Queensland University of Technology Human Ethics Committee approved aspirate collection (Ethics number: 1541A). A single puncture into the iliac crest was performed to collect 20 mL of BMA. BMA samples were diluted 1:1 with 2 mM EDTA/PBS and overlaid onto 15 mL Ficoll Paque Plus (GE Healthcare). The solution was centrifuged at 400 × g for 30 min. Interface cells were collected, washed and resuspended in low glucose DMEM (DMEM-LG; Gibco) containing 10% fetal bovine serum (FBS; Life Technologies), 10 ng/mL fibroblast growth factor-1 (FGF-1; Peprotech, Israel), and 100 U/ml penicillin/streptomycin (PenStrep; Gibco). The cells collected from the Ficoll separation of individual aspirates were seeded into three T175 flasks (Becton Dickinson, New Jersey USA), with 35 mL of culture medium per flask. The cultures were incubated overnight in a 20% O_2 and 5% CO_2 atmosphere at 37 °C. The next day, cultures were enriched for plastic adherent cells by aspirating off the medium containing non-adherent cells, and replacing with fresh culture medium. The cultures were then transferred to a reduced-O_2 incubator with a 2% O_2 and 5% CO_2 atmosphere at 37 °C. Adherent cells were passaged when the monolayer reached 80% confluency using 0.25% Trypsin/EDTA (Gibco). The cells were re-seeded at ~1500 cells per cm^2 in new culture flasks.

2.6. MSC flow cytometry characterization of MSC

Expanded cells were characterized for their expression of CD45, CD34, CD90, CD73, CD105, CD44, CD146, CD271 and HLA-DR (Miltenyi Biotec). The cells were stained with fluorescently conjugated antibodies as per manufacturer's instructions and analyzed on a BD LSRII flow cytometer (Becton Dickinson). Data was analyzed using FlowJo software (TreeStar, Oregon, USA).

2.7. Chondrogenic induction culture

To induce chondrogenic differentiation, MSC were resuspended in DMEM-high glucose (DMEM-HG; Gibco) containing, 1× GlutaMax (Gibco), 10 ng/mL TGF-β1 (PeproTech, Rocky Hill, NJ), 100 nM dexamethasone (Sigma), 200 μM ascorbic acid 2-phosphate (Sigma), 100 μM sodium pyruvate (Gibco), 40 μg/mL L-proline (Sigma), 1% ITS-X (Gibco) and 100 U/ml PenStrep (Gibco).

2.8. Control pellet culture

Control pellet cultures were prepared in 96-deep well V-bottom plates (Cat#: 3960, Corning) by suspending 2×10^5 MSC in 1 mL of chondrogenic induction medium. MSC were pelleted in the V-bottom plates by centrifuging the plate at 500 × g for 3 min. Induction cultures were maintained in a 2% O_2 and 5% CO_2 atmosphere at 37 °C. A half-volume medium exchange was performed every second day.

2.9. Cartilage microtissue manufacture in the microwell-mesh

The mechanism of depositing and retaining cells in the microwell-mesh is a key innovation in the current device. As shown schematically in Fig. 1C, cells can be directed through the 36 μm openings of the nylon mesh using centrifugation (forced aggregation [9]). Once the pelleted cells amalgamate, the resulting microtissues are too large (diameter >36 μm) to pass back through the pores of the nylon mesh, thereby retaining the microtissues in discreet microwells covered by the nylon mesh. All microwell-mesh cultures were performed in 6-well plates with 4 mL total chondrogenic induction medium per well. Prior to the addition of cells to the culture wells, 3 mL of cell-free chondrogenic induction medium was added to each well and the plate was centrifuged at 2000 × g for 2 min. This step was included to ensure bubbles were eliminated from the microwell-mesh prior to the addition of the cell inoculum. The cell inoculum was a 1 mL volume containing 1.2×10^6 MSC. As the microwell-mesh platform contained 240 microwells, this MSC concentration enabled the formation of microtissues containing ~5×10^3 cells each. MSC were pelleted in the microwell-mesh platform by centrifuging the plate at 500 × g for 3 min. Induction cultures were maintained in a 2% O_2 and 5% CO_2 atmosphere at 37 °C, with full-volume medium exchange performed every 2 days.

2.10. Microtissue harvest from the microwell-mesh

Microtissues were harvested from the microwell-mesh as shown schematically in Fig. 2. The microwell-mesh inserts were removed aseptically from the well plates using sterile forceps. The mesh was then gently peeled from the microwell insert using forceps. Nearly all of the cartilage microtissues remained loosely attached to the mesh. Microtissues were gently scraped off the mesh into a petri dish using a cell scraper (Cat#: 3011, Corning) and then collected into a 15 mL tube using PBS to resuspend.

2.11. Glucose uptake and lactic acid production

At each medium exchange time point, a portion of the spent medium was collected and stored at −80 °C for subsequent quantification of glucose and lactic acid concentration. Glucose and lactic acid analysis was performed by a pathology laboratory (Mater Hospital, Brisbane). Specific cellular uptake rates were determined based on the cell numbers used to initiate each culture and the glucose and lactic acid concentration at each medium exchange interval.

2.12. Glycosaminoglycan (GAG) quantification

GAG content was assessed in microtissues and pellets harvested on day 7, 14 and 21, as well as in media samples collected during media exchanges. All samples were stored at −80 °C until analysis. Microtissues or pellets were digested overnight at 60 °C using 1.6 U/mL papain (Sigma). DNA and GAG quantification was performed immediately after digestion (without freezing samples).

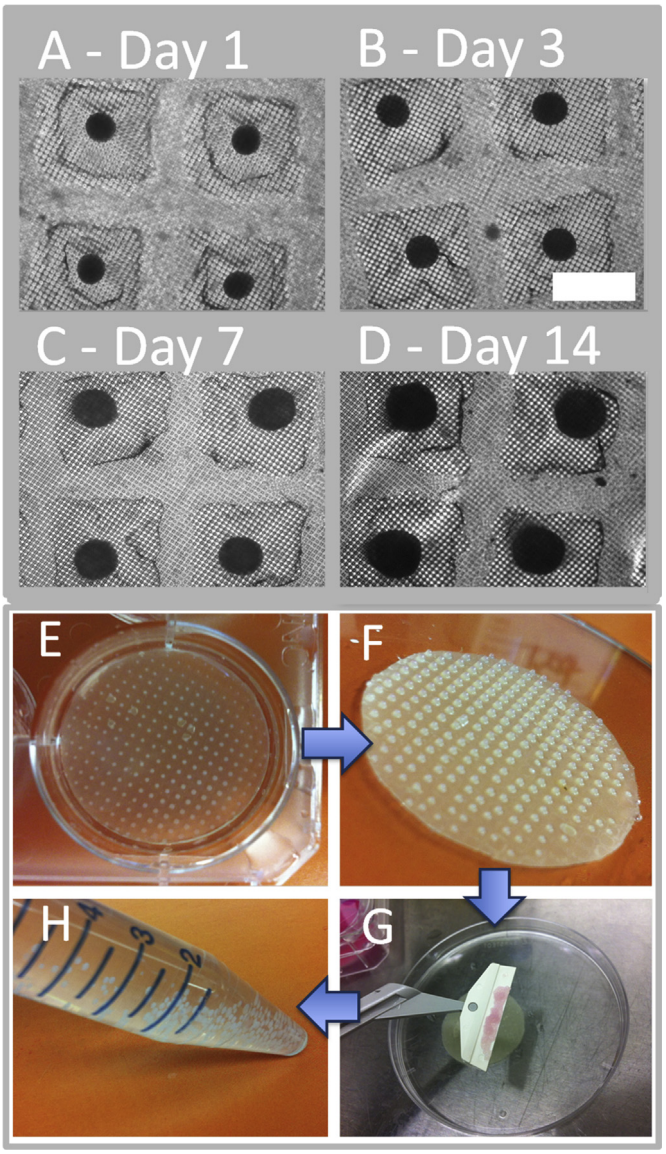

Fig. 2. (A–D) Microtissues increased in size during culture. (E) Following 21 days of culture, after 10 full medium exchanges, microtissues had been retained in discreet microwells by the nylon mesh. (F) Microwell-mesh inserts were removed from the well plates, and the nylon mesh was peeled from the PDMS insert. Most microtissues remained loosely bound to the mesh as shown in the image. (G&H) Cells were dislodged from the nylon mesh using a cell scraper and collected into a 15 mL tube containing PBS. Images A–D scale bar = 1 mm.

DNA content was determined using a PicoGreen assay kit (Life Technologies). GAG from tissue digests and medium were quantified using the 1,9-dimethymethylene blue (DMB, Sigma) assay as described previously [5]. Chondroitin sulfate sodium salt from shark cartilage (Sigma) was used to generate a standard curve for this assay. Data sets were analyzed for statistically significant differences in GAG levels between control cartilage pellets and microtissues at each time point using a two-tailed unpaired t-test, with significance indicated when $P < 0.05$.

2.13. Quantitative real-time RT-PCR (qRT-PCR)

RNA was isolated from control cartilage pellets and microtissues using the RNeasy Mini Kit (Qiagen) as per the manufacturer's instructions. Samples were subject to on-column DNase I digestion at

1 U/μL final concentration (Zymo Research). 60 ng of RNA was reverse transcribed using SuperScript III First-Strand Synthesis System for RT-PCR (Invitrogen) as per the manufacturer's instructions. For control cartilage pellets, a final amount of 60 ng of input RNA was achieved by pooling equal amounts of 2 independently generated pellets. 1 μL of the resultant cDNA product was used in a 20 μL qRT-PCR mastermix containing 1× SYBR Green PCR Master Mix (Applied Biosystems) and 200 nM each of the forward and reverse primers. 5 μL triplicate reactions were run in 384 well plates on a Viia7 Real Time PCR System (Applied Biosystems) as technical replicates. Run parameters were a single initial cycle of 50 °C for 2 min and 95 °C for 10 min, followed by 40 cycles of 95 °C for 15 s and 60 °C for 1 min. Specificity of products was confirmed by melt curve analysis. Three housekeeping genes (GAPDH, RPLPO and RPL13A) were analyzed for each sample. Relative gene expression for day 7 pellets was determined using GAPDH, while RPL13A was deemed the most stable housekeeping gene for the normalization of day 14 and day 21 samples. Data sets were analyzed for statistically significant differences in gene expression levels between control cartilage pellets and microtissues at each time point using a two-tailed, unpaired t-test with confidence intervals set at 95%. Primer sets used are detailed in Table 1. Previously published primers were as follows: GAPDH, ACAN, COL1A1, COL2A1 [14]; RPL13A, RPLPO and COL10A1 [15]; RUNX2 [16]. Primers for SOX9 were designed using Primer3Plus software [17].

2.14. Artificial cartilage defect model, fill and subcutaneous implantation

Artificial cartilage defect models were prepared from bovine tissue, filled with engineered control pellets or microtissues, sealed with fibrin glue, and then incubated subcutaneously in NOD/SCID mice. Similar cartilage defect models have been described previously [18]. While such models are not true representations of cartilage defects, they do provide reference bone/cartilage tissues and an indication of the capacity of the fill tissue to bond with native tissue(s). In our study, bovine legs, including the knee capsules, were purchased from G.E. Mallan Bulk Meats Fairfield (Australia). Plugs of cartilage and bone were drilled out from the knees using a 10 mm coring bit, and full thickness cartilage defects drilled out of the plug using a 3.5 mm drill bit (Fig. 7). Defect models were repeatedly washed in PBS to remove debris, and then sterilized in 70% ethanol/water for 2 h. Sterilized defect models were washed three times with PBS and then left to soak in PBS overnight to elute any remaining ethanol. Defect models were then frozen until time of use. Prior to loading the defect models with control cartilage pellets or microtissues, the models were soaked in chondrogenic induction medium for 20 min. Control pellets or microtissues that had been cultured in chondrogenic induction medium for 2 weeks were loaded into the defect sites using a transfer pipette (Sarstedt AG & Co. Sarstedt, Germany). The top of the defect was sealed using fibrin glue (Tisseel™, Baxter) by first dripping 20 μL of the fibrinogen solution over the defect, followed by 20 μL of thrombin solution. Defect models were then submerged in 1 mL of chondrogenic induction medium (in a 24-well plate) and incubated overnight in a 2% O_2 and 5% CO_2 atmosphere at 37 °C. After 24 h, the defect models were implanted subcutaneously into NOD/SCID mice. The University of Queensland and the Queensland University of Technology animal ethics committees approved this procedure. Two defect models were placed subcutaneously onto the back of each 8-week-old female mouse. The tissues were allowed to mature *in vivo* for 8 weeks at which point the animals were euthanized and the tissues explanted for analysis.

Table 1
Primers used for qRT-PCR.

Gene	Sequence (5′–3′)	Amplicon size (bp)
GAPDH		70
forward	ATGGGGAAGGTGAAGGTCG	
reverse	TAAAAGCAGCCCTGGTGACC	
ACAN		85
forward	TCGAGGACAGCGAGGCC	
reverse	TCGAGGGTGTAGCGTGTAGAGA	
COL1A1		83
forward	CAGCCGCTTCACCTACAGC	
reverse	TTTTGTATTCAATCACTGTCTTGCC	
COL2A1		79
Forward	GGCAATAGCAGGTTCACGTACA	
Reverse	CGATAACAGTCTTGCCCCACTT	
RPL13A		101
Forward	GGCTTTCCTCCGCAAGCGGAT	
Reverse	GCAGCATACCTCGCACGGTCC	
RPLPO		137
Forward	TGTGGGCTCCAAGCAGATGCA	
Reverse	GCAGCAGTTTCTCCAGAGCTGGG	
COL10A1		132
Forward	ACTCCCAGCACGCAGAATCCA	
Reverse	TGGGCCTTTTATGCCTGTGGGC	
RUNX2		133
Forward	GGAGTGGACGAGGCAAGAGTTT	
Reverse	AGCTTCTGTCTGTGCCTTCTGG	
SOX9		102
Forward	ACTCCTCCTCCGGCATGAG	
Reverse	GCTGCACGTCGGTTTTGG	

2.15. Histology and immunohistochemistry

Pellets and cartilage microtissues were fixed in 4% paraformaldehyde (PFA) for 30 min and frozen in Tissue-Tek OCT compound (Sakura Finetek) on days 7, 14 and 21. Samples were cryosectioned at 7 μm and collected onto poly-lysine coated slides (Thermo-Scientific, Waltham, MA) and frozen until further processing. Thawed sections were fixed for 20 min with 4% PFA and washed with PBS.

Explanted defect models were fixed in 4% PFA for 24 h and decalcified with decalcification solution (10% EDTA, 0.07% glycerol, PBS, pH 7.4) at 4 °C on a rocker, replacing the solution each day. Once the bone was pliable, the defect constructs were washed with PBS. The constructs were dehydrated in a graded series of ethanol and paraffin-embedded. 5 μm sections were cut in the sagittal plane. Sections were deparaffinized with xylene and rehydrated through a graded series of ethanol, and then stained with Alcian blue (Sigma–Aldrich) or Safranin-O (Sigma–Aldrich) to detect glycosaminoglycan (GAG) and with Nuclear Fast Red (Sigma–Aldrich) to detect nuclei.

Immunofluorescence (IF) staining was performed for collagen type I (Col I), collagen type II (Col II) and collagen type X (Col X). For Col II and Col X, sections were treated with chondroitinase (0.25 U/mL, Sigma) and hyaluronidase (2 U/mL, Sigma) for 60 min at 37 °C. For Col I, tissue sections were treated with Proteinase K (2.0 μg/mL) for 15 min. Sections were permeabilized with 0.1% Triton X-100 for 5 min and blocked with 10% normal goat serum (Invitrogen) for 30 min at room temperature. The sections were then stained with primary antibodies (all from Abcam) raised against Col I (1:800; Cat# ab6308), Col II (1:100; Cat# ab34712) and Col X (1:100; Cat# ab58632) in 1% BSA/PBST (PBS + 0.1% Tween 20) at 4 °C overnight. Secondary antibody detection was performed using Alexa Fluor 568-conjugated goat anti-rabbit IgG and Alexa Fluor 488-conjugated goat anti-mouse IgG (both from Molecular Probes) at 1:1000 in 1% BSA/PBS for 60 min at room temperature in the dark. After each staining step, unbound antibodies were washed 3 times with PBS for 5 min each. Nuclei were counterstained with DAPI (Molecular Probes) for 5 min at room temperature in the dark.

Sections were mounted with ProLong Gold antifade reagent (Molecular Probes) and examined with an Olympus BX61 fluorescence microscope. Negative controls were prepared the same as above, but without primary antibodies.

3. Results

3.1. Microwell-mesh characterization via micro-computed tomography (mCT)

mCT characterization of the microwell-mesh surface and cross-section demonstrated that the dimensions of the microwell mold were reliably cast into the PDMS negative. The nylon mesh sealed each individual microwell, forming individual v-bottom microwells that were 2 mm × 2 mm square × 0.8 mm deep.

3.2. MSC flow cytometry characterization

As shown in Supplementary Fig. 1, MSC stained negative for hematopoietic markers CD45 and CD34 and positive for MSC markers CD90, CD44, CD73, CD105, CD146. Approximately 12% of cells were CD271 positive.

3.3. Microwell-mesh tissue retention over extended culture

Fig. 2A–D shows the growth of the cartilage microtissues in the microwell-mesh over the first 14 days culture period prior to *in vivo* implantation. Cartilage microtissues were retained within the microwell-mesh over the 21 day culture period (Fig. 2E). No microtissues were displaced from microwells despite 10 full medium exchanges. When the mesh was peeled away from the microwell platform (Fig. 2F), nearly all of the microtissues remained loosely attached to the mesh and were easily harvested by gentle scraping (Fig. 2G&H). The image of the mesh at day 21 (Fig. 2E&F) illustrates the uniformity of the microtissues manufactured using the microwell-mesh platform.

3.4. Glucose uptake and lactic acid production

Microwell-mesh cultures were initiated with 1.2×10^6 cells in 4 mL of medium, and control pellet cultures were initiated with 2×10^5 cells in 1 mL of medium. In order to provide similar rates of medium exchange, full-volume medium exchanges were performed on microwell-mesh cultures and half-volume medium exchanges were performed on control pellet cultures every 2 days. The measured glucose consumption and the accumulation of lactic acid between medium exchanges is shown graphically in Fig. 3A and C, respectively. The microwell-mesh cultures exhibited more rapid fluctuation in medium glucose and lactic acid content between medium exchanges. The glucose concentration in the microwell-mesh cultures declined from ~22 mM to ~10 mM at each medium exchange, and there was a corresponding increase in lactic acid concentration to approximately 25 mM. Fig 3B shows that the specific cellular glucose uptake rates in the microwell-mesh cultures and control pellet cultures were $7.28 \times 10^{-10} \pm 9.1 \times 10^{-11}$ mmol/cell/hour and $1.17 \times 10^{-10} \pm 2.5 \times 10^{-11}$ mmol/cell/hour, respectively. This data indicates that the specific cellular glucose uptake rates in the microwell-mesh cultures were approximately 6.2-fold greater than in the control pellet cultures. Similar glucose uptake rates have been reported for chondrocytes in cartilage [19], and very similar rates (3.57×10^{-10} mmol/cell/hour) have been reported for pellet cultures formed from 2×10^5 MSC each [20].

Fig 3D shows that the specific cellular lactic acid production rates in the microwell-mesh cultures and control pellet cultures were $1.60 \times 10^{-9} \pm 2.9 \times 10^{-11}$ mM/cell/hour and $2.34 \times 10^{-10} \pm 4.9 \times 10^{-11}$ mM/cell/hour, respectively. This suggests that the specific cellular lactic acid production rates in the microwell-mesh culture were ~6.8-fold greater than in the control pellet cultures. The ~2:1 ratio of glucose consumption to lactic acid production indicates that cells in both culture systems were largely respiring anaerobically.

3.5. GAG secretion profiles

DNA quantity was used as an indirect measure of cell number at various time-points. We observed a reduction in DNA in both the control pellet cultures and microwell-mesh cultures. The DNA content in the cultures dropped between culture initiation and day 7, after which the DNA content remained stable in all cultures (Fig. 4A). Total cell secreted GAG was quantified using a medium sample collected at each media exchange interval. The quantity of GAG in the cartilage microtissue culture medium was greater than in the control pellet culture medium at all medium exchange time points (Fig. 4B). The quantity of GAG secreted by the microwell-mesh cultures increased rapidly over the first 6 days of culture, stabilized at 35–45 μg GAG/μg DNA during the second week of culture, and then dropped marginally to ~30 μg GAG/μg DNA over the third week of culture. By contrast the control pellet cultures secreted ~10 μg GAG/μg DNA at day 6, with this value increasing to ~17 μg GAG/μg DNA over the second week, after which it stabilized at ~15 μg GAG/μg DNA over the third week of culture.

3.6. GAG retained in tissues

The quantity of GAG retained in tissues was standardized to the corresponding DNA content at the point of harvest (Fig. 4A). Tissue-retained GAG per μg DNA in the microwell-mesh cultures always exceeded the tissue-retained GAG in control pellet cultures (Fig. 4C). The relative tissue-retained GAG per μg DNA was 7.8-fold, 1.7-fold and 1.3-fold greater in the microwell-mesh culture than in the control pellet culture at day 7, day 14 and day 21, respectively.

3.7. Chondrogenic and hypertrophic gene expression

In vitro cultured cartilage tissues were analyzed for expression of genes related to both chondrogenesis and hypertrophy (Fig. 5). In the first two weeks of culture, microwell-mesh tissues tended to express higher levels of the chondrogenic genes SOX9, collagen II and aggrecan, as compared to control pellet tissues at similar time points. These differences were only statistically significant for collagen II at days 7 and 14, and for aggrecan at day 7. By day 21 this trend appeared to be reversing with little difference detected between the two culture conditions for collagen II and aggrecan, and significantly greater levels of SOX9 in the control pellet tissues, compared to the microwell-mesh tissues. Markers of hypertrophy, RUNX2 and collagen X, were expressed at significantly higher levels in microwell-mesh tissues compared to control pellet culture tissues at all time points with the exception of RUNX2 at day 7. Collagen I, a marker of fibrocartilage or bone formation, was also detected at significantly higher levels in the microwell-mesh cartilage tissues at day 7 and 14, but not at day 21 when compared to control pellet culture tissues.

3.8. In vitro histology and matrix characterization

Histological sections from cartilage tissue produced in the microwell-mesh and control pellet cultures at day 7, 14 and 21 are shown in Fig. 6. Alcian blue staining shows that the GAG content was greater and more evenly distributed in cartilage microtissues at

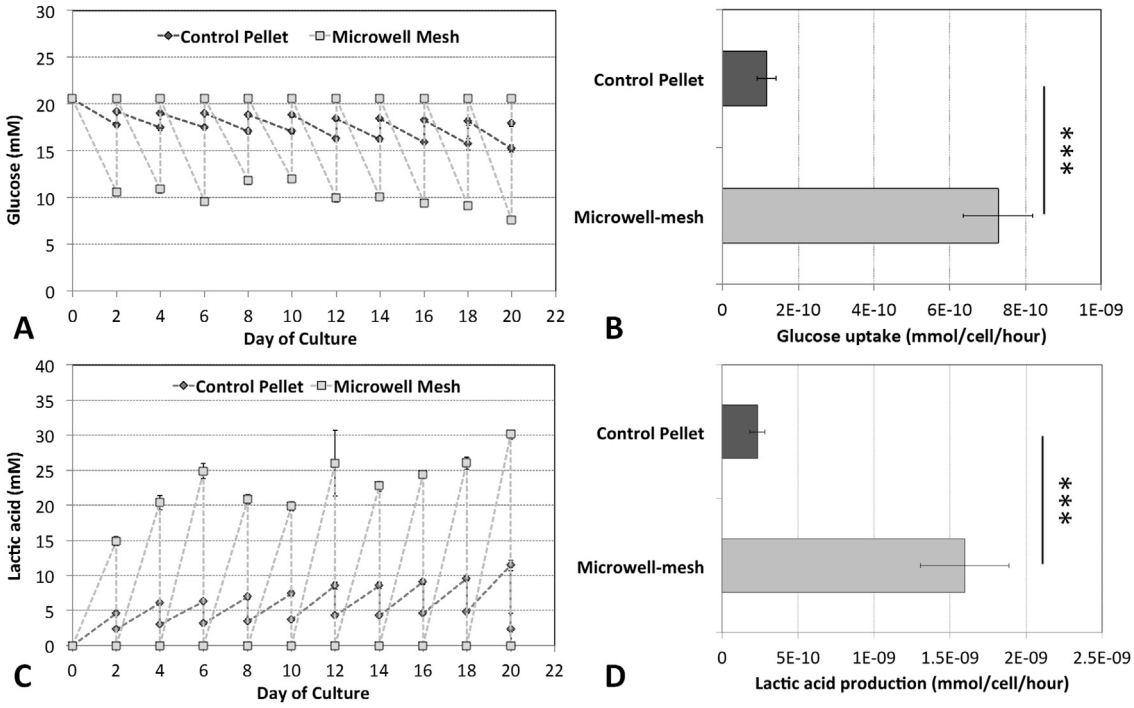

Fig. 3. Glucose uptake and lactic acid production rates were estimated following the quantification of glucose and lactic acid concentrations in the medium at medium exchange intervals. (A&C) Glucose and lactic acid concentrations in remaining in medium samples taken at exchange intervals were quantified. (B&D) The specific cellular uptake of glucose and lactic acid production rates were estimated based on the concentrations shown in captions A&C and the cell number used to initiate the control pellet and microwell-mesh cultures, respectively (mean ± SD, n = 6, $P < 0.05$).

day 7 relative to control cartilage pellets. The intense and uniform distribution of Alcian blue staining in the cartilage microtissues persisted at day 14 and day 21. By contrast, the intensity of Alcian blue staining of the control cartilage pellets was very weak at day 7, but increased substantially over the next two weeks (day 14 and day 21), with staining intensity matching that of the microtissues by day 21.

The cores of control pellet cartilage tissues at day 7 were completely devoid of collagen II staining. In contrast, cartilage microtissues expressed collagen II throughout the entirety of the majority of pellets, with evidence of increased expression at the periphery. By day 14 both control cartilage pellets and cartilage microtissues expressed collagen II throughout the tissues, with distinctly stronger staining at the periphery. This pattern of expression was maintained at day 21 for both the control pellet tissues and the cartilage microtissues.

Similar to collagen II expression, collagen X staining was absent in the core of control pellet tissues at day 7. Cartilage microtissues at day 7 showed uniform collagen X staining with no evidence of increased levels at the periphery of the tissues. At days 14 and 21 the pattern of collagen X expression was reminiscent of that observed for collagen II expression for both tissue types, with expression throughout the tissues and more intense staining at the periphery.

Collagen I was expressed throughout the cartilage microtissues at day 7 with a consistently increased level of expression at the outer edges of the tissues. As with the other collagens, day 7 control cartilage pellets were completely devoid of staining in the central zone with expression restricted to the periphery of the tissues. Under both culture conditions, there was evidence of more uniform expression throughout the tissues at day 14. By day 21 collagen I expression was becoming increasingly restricted to the periphery of both cartilage microtissues and control pellet cartilage tissues.

3.9. *In vivo* histology and matrix characterization

Control cartilage pellets and cartilage microtissues that had been cultured in chondrogenic induction medium for 14 days were used to fill cartilage defect models and implanted subcutaneously into NOD/SCID mice for 8 weeks. Harvested explants were sectioned and stained to characterize the fill of the cartilage defect model and the matrix distribution in the matured cartilage tissues (Fig. 7). As expected, the smaller cartilage microtissues packed into defects more efficiently, compared to the larger diameter control cartilage pellets. Both the control cartilage pellets and cartilage microtissues integrated with the native tissue of the defect model, requiring significant force to remove them from the defect site. Individual pellets also bonded together during the *in vivo* incubation period, producing as a single unit if removed from the defect site.

Upon dissection it was evident that multiple cartilage tissues had bonded together during the *in vivo* incubation period. However, both the control pellet tissues and the cartilage microtissues retained discrete pellet morphology with central areas of each pellet displaying high levels of proteoglycans and significant GAG content (Fig. 7 Safranin-O and Alcian blue respectively). High levels of the chondrogenic marker collagen II were detected in both the native tissue of the defect model and in the engineered tissues. This was offset by the presence of collagen I staining predominantly at the periphery of the control cartilage pellets and cartilage microtissues indicating the formation of fibrocartilage or bone-like tissue.

4. Discussion

Cartilage pellet cultures were first described in 1998 [21] and traditionally involve the aggregation of $1–5 \times 10^5$ MSC in chondrogenic induction medium. This MSC chondrogenic differentiation

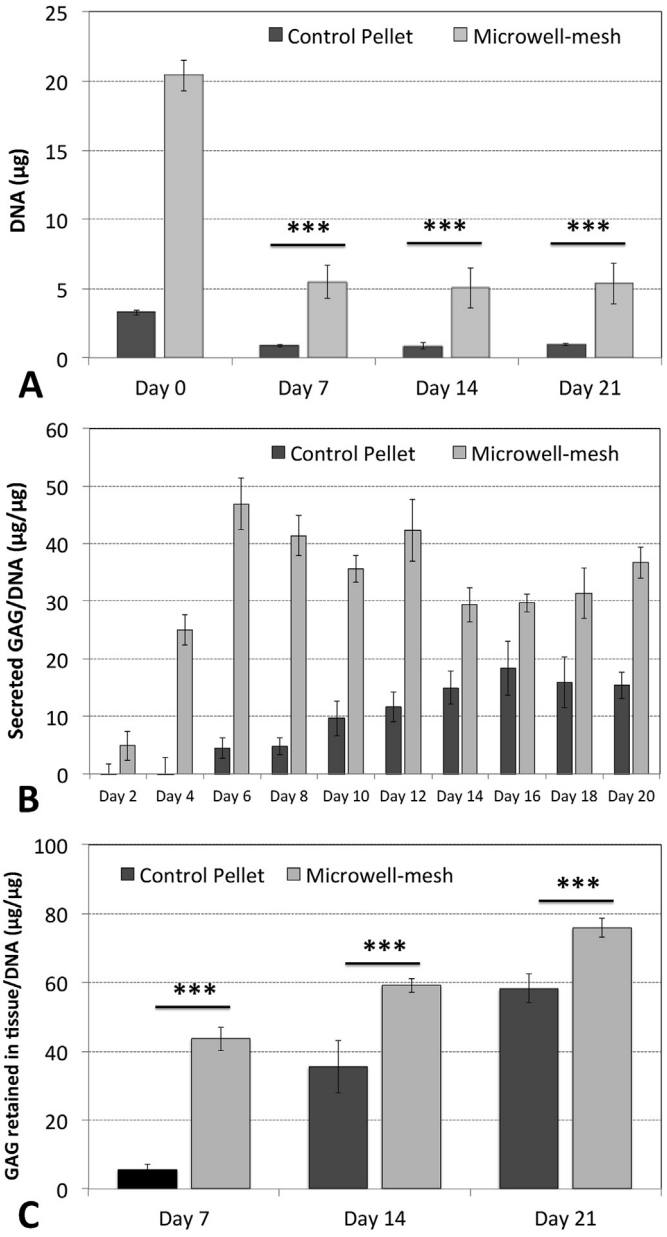

Fig. 4. DNA in harvested tissues, and GAG secretion into medium and GAG retained in Microwell-mesh and pellet cultured tissues. (A) Total DNA content (μg) detected for each culture was proportional to the initial number of cells seeded. Control pellet cultures were initiated with 2×10^5 cells each, while microwell-mesh cultures were initiated with 1.2×10^6 cells each. (B) The GAG secreted by cultures maintained microwell-mesh as a function of the tissue DNA content was greater than in the control cartilage pellet cultures. (C) The quantity of retained GAG per μg of DNA was greater in microwell-mesh cartilage microtissues than in control pellet cartilage tissues at each time point (mean ± SD, n = 6, $P < 0.05$).

platform and cartilage-like tissue manufacturing approach remains gold standard in the field. While reasonably effective, the resulting large diameter (2–3 mm) pellets form steep radial diffusion gradients [5]. Radial heterogeneity in both cell phenotype and matrix composition is common [22,23] and a necrotic core is sometimes observed [24].

We have previously manufactured thousands of smaller diameter cartilage microtissues using the Aggrewell™ (StemCell Technologies) [5] and our own in-house fabricated microwell platform [8]. The reduced diameter enhanced metabolite and signal molecule diffusion in the resulting microtissues, enabled the formation of more homogenous tissue, and significantly enhanced chondrogenic differentiation [5]. While this demonstrated the advantages of cartilage microtissues over traditional cartilage pellets, integrating more sophisticated medium exchange and scale-up protocols was frequently thwarted by the displacement of microtissues from their original discrete microwells. Displaced microtissues were either lost from culture or redistributed into adjacent microwells and amalgamated with other microtissues. To overcome this technical barrier, we developed the microwell-mesh platform. In this paper we used the microwell-mesh to manufacture microtissues from 5×10^3 MSC each. This cell number was selected through preliminary experimentation that demonstrated that cartilage microtissues of this size grew to fill the 2 mm × 2 mm × 0.8 mm microwells (as shown in Fig. 2) over the given culture period, and that microtissues of this size could be easily harvested for downstream processing. Today, soft lithography and other industrial fabrication methods make the manufacture of microwell-mesh platforms with a range of microwell dimensions readily achievable. The size of resultant microtissues can be readily controlled by tailoring the size of the microwells or the number of cells loaded in the microwells. Smaller microwells are more suitable for the manufacture of smaller microtissues, described in previous papers [4,5,7,8]. The platform designed and tested here is suitable for producing microtissues starting from cell numbers of >1000 cells per microtissue or microtissues that may grow substantially during the culture period from fewer cells. The suitability of a specific shape/size of microwell system and the cell-to-microwell seeding ratio should be considered a critical experimental design consideration, as these factors can affect culture outcomes, including including cell differentiation [25]. The microwell-mesh dimensions described here are ideal for the formation and growth of MSC differentiated cartilage microtissues from 5×10^3 cells each. Attachment of a nylon mesh to enclose each microwell facilitated the retention of microtissues in discrete microwells during numerous full-medium exchanges over a 21-day culture period (Fig. 2). The mature microtissues were easily harvested by peeling the mesh from the PDMS microwell insert (Fig. 2).

Glucose uptake and lactic acid production rates were approximately 6-fold greater for cells cultured as microtissues in the microwell-mesh than cells in control pellet cultures (see Fig 3). These highly metabolically active cultures may benefit from more frequent media exchanges that could be facilitated by a perfusion feeding system. Because the mesh effectively retains microtissues within discrete microwells, this platform is well suited for integration with perfusion technologies. In this proof-of-concept study, we fully exchanged the 4 mL medium volume in microwell-mesh cultures every 2 days. Glucose turnover in control pellet cultures was comparatively minute, suggesting that the dimensions of the macroscopic pellet limit metabolism. Similarly, the increase in metabolic activity observed in the microwell-mesh cultures correlates with the observed accelerated chondrogenic differentiation and matrix development discussed below.

The accumulation of GAG and aggrecan in engineered tissues is associated with the early stages of MSC chondrogenesis [26]. Aggrecan is the primary proteoglycan in articular cartilage to which GAG side chains are linked, and these hybrid molecules are largely responsible for the compressive stiffness properties of articular cartilage [27,28]. Thus the rapid accumulation of GAG (Fig. 4B and C) and the early upregulation of aggrecan gene expression (Fig. 5) indicated accelerated chondrogenic differentiation in the microwell-mesh cultures, relative to the larger diameter control pellets. The comparatively low levels of GAG observed in the control pellets at day 7 (Fig. 4C) was consistent with Alcian blue histological staining (Fig. 6 – day 7), which suggested that GAG matrix accumulation was restricted to the periphery of these larger tissues.

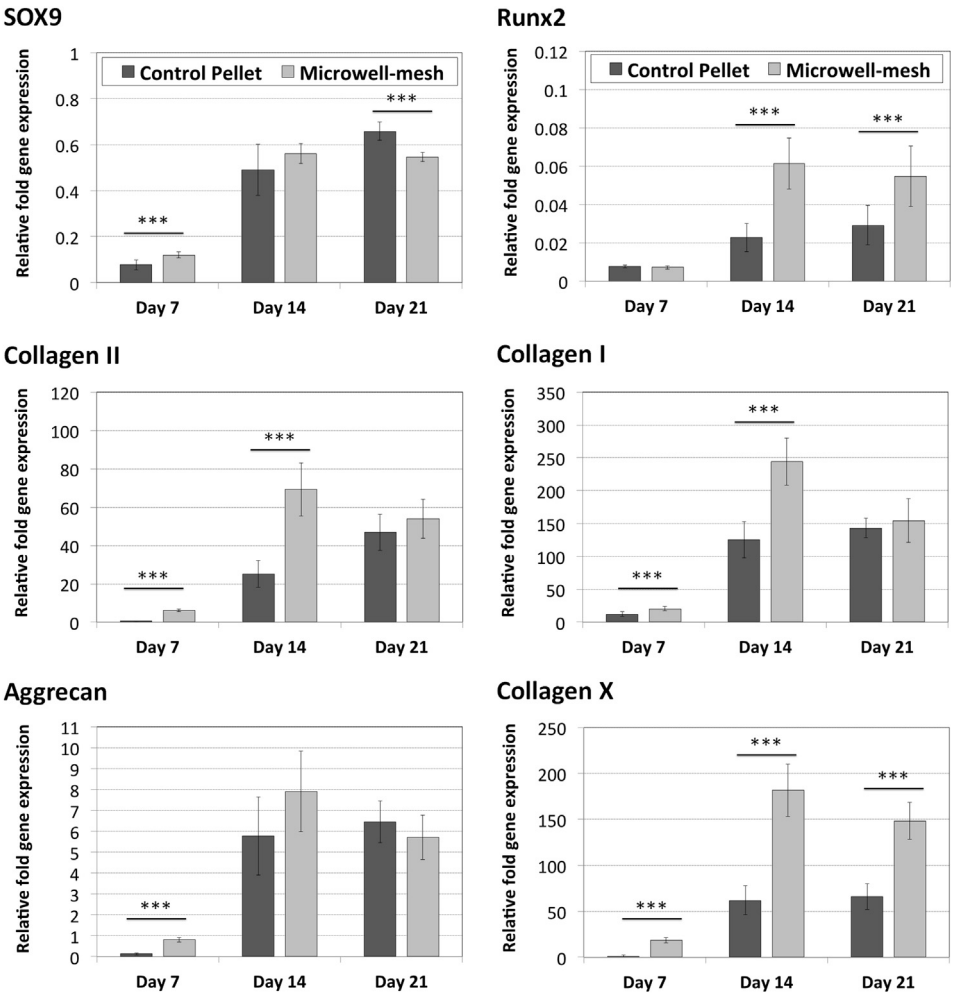

Fig. 5. qRT-PCR analysis of cartilage tissue produced by control pellet culture and microwell-mesh culture methods. Increased expression of chondrogenic markers was accompanied by increases in markers of hypertrophy and fibrocartilage formation in microwell-mesh cartilage tissues. Expression levels for day 7 samples are shown relative to GAPDH and for day 14 and 21 samples relative to RPLPO (plotted as mean ± SD, n = 3 for control pellet tissues and n = 4 for microwell-mesh tissues, *** indicates $P < 0.05$).

The accelerated cartilage microtissue MSC differentiation profile was supported by the more uniform collagen II matrix staining at day 7 relative to the control cartilage pellets (Fig. 6). As with the GAG profile, collagen II staining was only detectable at the periphery of the control cartilage pellets at day 7. The increased collagen II matrix staining by day 14 suggested that a wave of differentiation occurred in the control cartilage pellet, beginning at the periphery and progressing to the core. Increased levels of the SOX9, collagen II and aggrecan in microwell-mesh tissues at day 7 were again consistent with an earlier induction of chondrogenic signaling in the cartilage microtissues (Fig. 5). Taken together, the GAG analysis, collagen II staining and gene expression data cumulatively suggest that the cartilage microtissues matured more rapidly and in a more uniform manner than control cartilage pellets. The caveat of accelerated chondrogenic induction in cartilage microtissues, however, is an accelerated onset of hypertrophic features. RUNX2 and collagen X, both markers of hypertrophy, were expressed at greater levels in the microtissues when compared to the control cartilage pellets (Fig. 5). The only exception was RUNX2 at day 7, in which no difference was observed. Collagen I levels also suggested a propensity for cartilage microtissues to produce a more fibrous cartilage or to progress towards bone-like tissue, a less desirable trait in repair cartilage [11].

Filling defects with cartilage spheroids is a promising clinical strategy. Co.donAG (Germany) is currently evaluating the use of articular chondrocyte-derived pellets to repair cartilage defects in clinical trials [29]. We found that smaller diameter cartilage microtissues were able to more efficiently fill our cartilage defect model than larger control pellets (Fig. 7), as smaller packing material enables more efficient filling and reduced void space. Unfortunately, mineralization and hypertrophy remained the primary obstacles, as cartilage-like matrix, including GAG and proteoglycan, were restricted to the cores of individual pellets. Both control pellets and microtissues appeared to have a halo of hypertrophic tissue around the outside of the tissue. In this case the greater dimensions of the pellet cultures appeared enable the maintenance of larger tissue cores that retained detectable GAG and proteoglycan content (Fig. 7). The microtissues bonded strongly with the underlying bone, but poorly to the native cartilage that formed the walls of the defect model. The poor integration of both the pellets and the microtissues with the native cartilage was unsurprising given that the processing (ethanol sterilization and freezing) of the tissue to produce the defect is unlikely to leave viable tissue. Nevertheless, the poor integration between the pellets themselves remains problematic, and reflects the propensity for MSC-derived tissues to produce a calcified tissue, rather than a uniform matrix with cartilage-like properties. In recent work, we demonstrated that microtissues formed from articular chondrocytes readily amalgamated into a continuous macrotissue *in vitro* [8]. In order for MSC-differentiated cartilage tissues to progress into the clinic,

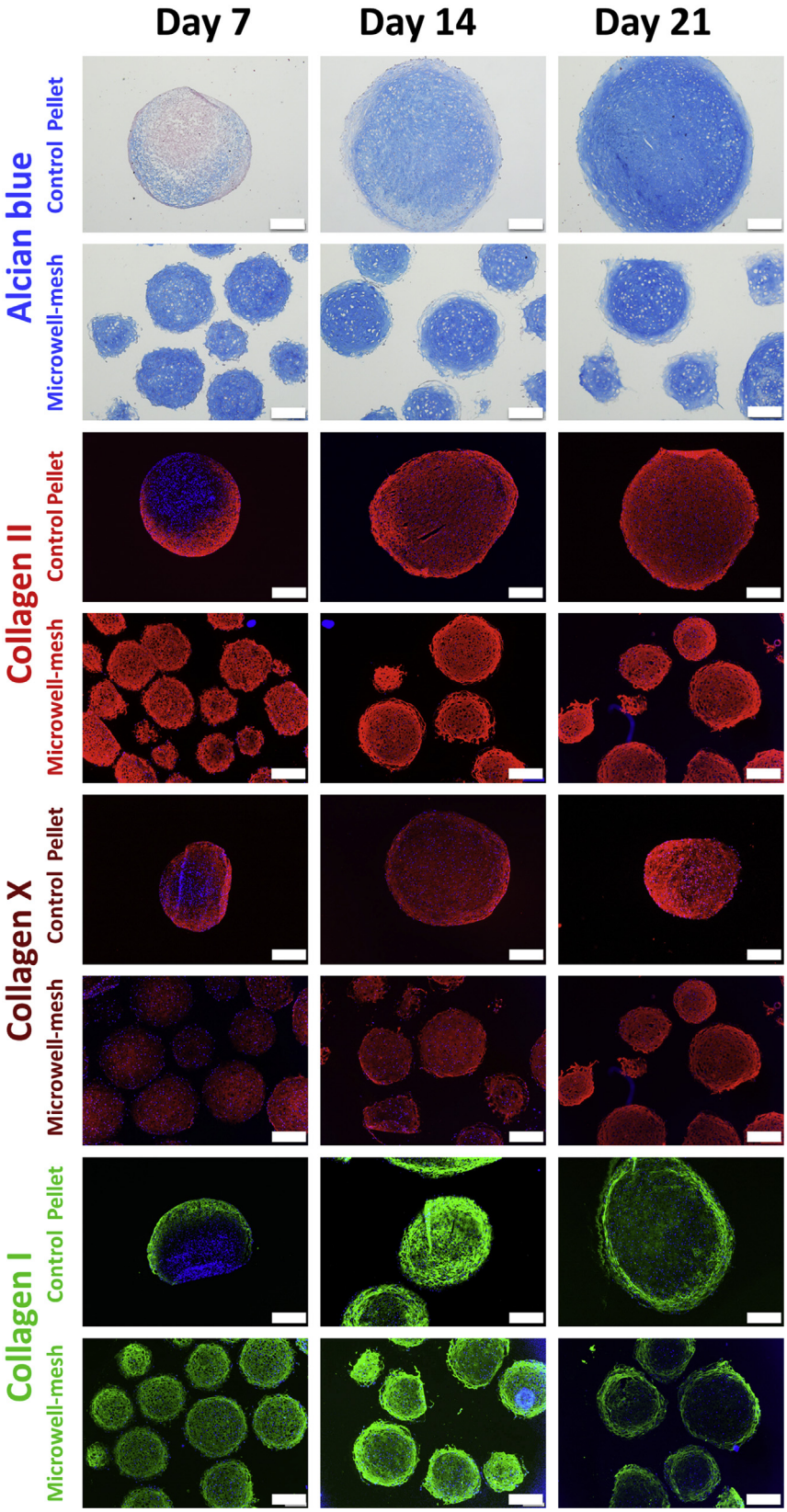

Fig. 6. GAG and collagen staining of cartilage tissues from the microwell-mesh and control pellet cultures. Tissues were counterstained for nuclei visualization with Nuclear Fast Red for Alcian blue stain and DAPI (blue) for immunofluorescent imaging of the collagens. Scale bars = 250 μm.

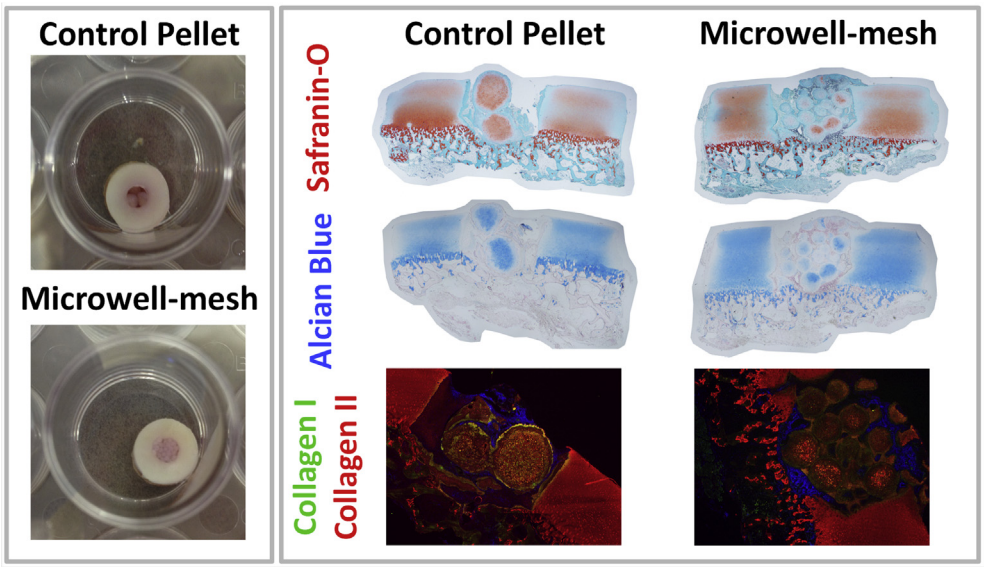

Fig. 7. Cartilage defect models were filled with either control cartilage pellets or microwell-mesh cartilage tissues, sealed with fibrin glue and subcutaneously implanted into NOD/SCID mice. Explant cartilage defect models were decalcified, sectioned and stained for proteoglycan content (Safranin-O), GAG content (Alcian blue), evidence of chondrogenesis (collagen II) and formation of fibrocartilage or bone (collagen I).

effective mitigation of hypertrophic tissue formation must be achieved.

Unfortunately, generating cartilage-like tissue from MSC remains challenging, with no current protocol capable of generating functional articular hyaline cartilage and chondrocytes that do not exhibit a hypertrophic phenotype [11]. We reasoned that the large-diameter control pellet cultures provide low-resolution heterogeneous readouts, confound efforts to optimize *in vitro* chondrogenic protocols, and make it difficult to characterize chondrogenic differentiation kinetics. We show here that microtissues generate a much more homogenous tissue in the first week of culture, and that the chondrogenic differentiation kinetics are likely more rapid than could be interpreted from control pellet culture data. It is therefore likely that the more homogenous microtissues will provide a higher resolution readout of MSC differentiation kinetics. In previous studies, control pellet cultures were exposed to chondrogenic induction medium for 14–21 days, followed by medium supplemented with parathyroid hormone-like peptide to mitigate hypertrophy [30,31]. The selection of the 14–21 day time points reflect assumed peaks in chondrogenic gene expression and the onset of hypertrophic features. Our data suggest that day 14 may represent a key inflection point in control pellet cultures (Fig. 5), at which intervention to block hypertrophic processes might be effective. However, the microtissue GAG secretion profiles (Fig. 4B&C), histological immunohistochemistry (Fig. 6), and gene expression analysis (Fig. 5) suggest that chondrogenesis may have peaked earlier, and that mitigation of hypertrophic onset may be required as early as at day 7. Early chondrogenesis and hypertrophy were also evident at the periphery of the control pellets as early as day 7 (Fig. 6), although not as clear as in cartilage microtissues at the same time point. The heterogeneity and delay in tissue maturation within the core of the control pellet (Fig. 6) confounded quantification of the differentiation kinetics by bulk gene expression (Fig. 5). We suggest that the bulk gene expression in the more homogeneous microtissues better represents MSC differentiation kinetics. The rapid differentiation kinetics observed in microtissues are likely comparable to the differentiation kinetics observed in the periphery of the control pellets. The more homogeneous microtissues should ultimately enable superior characterization of MSC differentiation kinetics, and better direct the timing of effective medium supplementation with parathyroid hormone-like peptide or other factors that mitigate hypertrophy.

While we applied the microwell-mesh concept to the manufacture of cartilage microtissues, we anticipate that this platform will have more general utility in 3D cell culture applications. This system will be particularly useful for drug screening and body-on-a-chip applications where 3D microtissues are increasingly viewed as superior *in vitro* model systems [1,3]. As multiple medium exchanges are required to replicate fluctuations in systemic drug concentration with time, or sequential treatment with a series of drugs, the microwell-mesh platform ensures replication of similar cyclical events or sequential treatments without displacing microtissues.

5. Conclusion

Microtissues are an increasingly favored *in vitro* tissue mimics for drug testing, studying developmental processes, and manufacturing building blocks for tissue engineering [3]. Herein, we described the fabrication protocol of a novel microwell platform using readily accessible materials and equipment; the ***microwell-mesh***. The microwell-mesh platform, which retained microtissues within discrete microwells, enabled the efficient manufacture and retention of MSC-derived cartilage microtissues in discrete microwells over a 21-day culture period that included multiple full-volume media exchanges. Cartilage-like matrix formation was more rapid and homogeneous in microtissues than in conventional large diameter control cartilage pellets. The more homogenous matrix formation observed in the cartilage microtissues may provide a high-resolution tool to optimize chondrogenic medium formulations and the culture conditions necessary to mitigate hypertrophy and generate hyaline cartilage. Retention of the microtissues within discrete microwells make the microwell-mesh platform an ideal tool for the high-throughput optimization of cartilage microtissue culture conditions. While we focused on manufacturing cartilage microtissues, we anticipate that the microwell-mesh platform will have broader utility in the manufacture of other tissue mimics and cancer models.

Acknowledgments

The authors would like to thank the National Health and Medical Research Council (NHMRC) of Australia and Inner Wheel Australia for their support, Dr Betul Babur for assistance with the hotpress fabrication of some of the molds, Dr Nathan Boase for assistance with the microCT imaging, and Ms Josephine Tarren for assistance with the glucose & lactic acid quantification.

Appendix A. Supplementary data

Supplementary data related to this article can be found at http://dx.doi.org/10.1016/j.biomaterials.2015.05.013.

References

[1] T. Jacks, R.A. Weinberg, Taking the study of cancer cell survival to a new dimension, Cell 111 (2002) 923–925.
[2] F. Langenbach, K. Berr, C. Naujoks, A. Hassel, M. Hentschel, R. Depprich, et al., Generation and differentiation of microtissues from multipotent precursor cells for use in tissue engineering, Nat. Protoc. 6 (2011) 1726–1735.
[3] E. Fennema, N. Rivron, J. Rouwkema, C. van Blitterswijk, J. de Boer, Spheroid culture as a tool for creating 3D complex tissues, Trends Biotechnol. 31 (2013) 108–115.
[4] K.F. Chambers, E.M. Mosaad, P.J. Russell, J.A. Clements, M.R. Doran, 3D cultures of prostate cancer cells cultured in a novel high-throughput culture platform are more resistant to chemotherapeutics compared to cells cultured in monolayer, PloS one 9 (2014) e111029.
[5] B.D. Markway, G.K. Tan, G. Brooke, J.E. Hudson, J.J. Cooper-White, M.R. Doran, Enhanced chondrogenic differentiation of human bone marrow-derived mesenchymal stem cells in low oxygen environment micropellet cultures, Cell. Transplant. 19 (2010) 29–42.
[6] M. Kabiri, B. Kul, W.B. Lott, K. Futrega, P. Ghanavi, Z. Upton, et al., 3D mesenchymal stem/stromal cell osteogenesis and autocrine signalling, Biochem. Biophysical Res. Commun. 419 (2012) 142–147.
[7] M.M. Cook, K. Futrega, M. Osiecki, M. Kabiri, B. Kul, A. Rice, et al., Micromarrows-three-dimensional coculture of hematopoietic stem cells and mesenchymal stromal cells, Tissue Eng. Part C. Methods 18 (2012) 319–328.
[8] B.K. Babur, P. Ghanavi, P. Levett, W.B. Lott, T. Klein, J.J. Cooper-White, et al., The interplay between chondrocyte redifferentiation pellet size and oxygen concentration, PloS one 8 (2013) e58865.
[9] M.D. Ungrin, C. Joshi, A. Nica, C. Bauwens, P.W. Zandstra, Reproducible, ultra high-throughput formation of multicellular organization from single cell suspension-derived human embryonic stem cell aggregates, PloS one 3 (2008) e1565.
[11] R.A. Somoza, J.F. Welter, D. Correa, A.I. Caplan, Chondrogenic differentiation of mesenchymal stem cells: challenges and unfulfilled expectations, Tissue Eng. Part B Rev. 20 (2014) 596–608.
[12] L. Gitlin, P. Schulze, D. Belder, Rapid replication of master structures by double casting with PDMS, Lab a Chip 9 (2009) 3000–3002.
[13] R.D. Misra, P.M. Chaudhari, Osteoblasts response to nylon 6,6 blended with single-walled carbon nanohorn, J. Biomed. Mater. Res. Part A 101 (2013) 1059–1068.
[14] I. Martin, M. Jakob, D. Schafer, W. Dick, G. Spagnoli, M. Heberer, Quantitative analysis of gene expression in human articular cartilage from normal and osteoarthritic joints, Osteoarthr. Cartilage/OARS, Osteoarthr. Res. Soc. 9 (2001) 112–118.
[15] E. Ragni, M. Vigano, P. Rebulla, R. Giordano, L. Lazzari, What is beyond a qRT-PCR study on mesenchymal stem cell differentiation properties: how to choose the most reliable housekeeping genes, J. Cell. Mol. Med. 17 (2013) 168–180.
[16] N. Selvamurugan, S. Kwok, N.C. Partridge, Smad3 interacts with JunB and Cbfa1/Runx2 for transforming growth factor-beta1-stimulated collagenase-3 expression in human breast cancer cells, J. Biological Chem. 279 (2004) 27764–27773.
[17] A. Untergasser, I. Cutcutache, T. Koressaar, J. Ye, B.C. Faircloth, M. Remm, et al., Primer3—new capabilities and interfaces, Nucleic Acids Res. 40 (2012) e115.
[18] G.C. Schuller, B. Tichy, Z. Majdisova, T. Jagersberger, M. van Griensven, S. Marlovits, et al., An in vivo mouse model for human cartilage regeneration, J. Tissue Eng. Regen. Med. 2 (2008) 202–209.
[19] H.K. Heywood, D.L. Bader, D.A. Lee, Rate of oxygen consumption by isolated articular chondrocytes is sensitive to medium glucose concentration, J. Cell. Physiology 206 (2006) 402–410.
[20] G. Pattappa, H.K. Heywood, J.D. de Bruijn, D.A. Lee, The metabolism of human mesenchymal stem cells during proliferation and differentiation, J. Cell. Physiol. 226 (2011) 2562–2570.
[21] B. Johnstone, T.M. Hering, A.I. Caplan, V.M. Goldberg, J.U. Yoo, In vitro chondrogenesis of bone marrow-derived mesenchymal progenitor cells, Exp. Cell. Res. 238 (1998) 265–272.
[22] F. Barry, R.E. Boynton, B. Liu, J.M. Murphy, Chondrogenic differentiation of mesenchymal stem cells from bone marrow: differentiation-dependent gene expression of matrix components, Exp. Cell. Res. 268 (2001) 189–200.
[23] T.Y. Hui, K.M.C. Cheung, W.L. Cheung, D. Chan, B.P. Chan, In vitro chondrogenic differentiation of human mesenchymal stem cells in collagen microspheres: influence of cell seeding density and collagen concentration, Biomaterials 29 (2008) 3201–3212.
[24] R.S. Tare, D. Howard, J.C. Pound, H.I. Roach, R.O. Oreffo, Tissue engineering strategies for cartilage generation – micromass and three dimensional cultures using human chondrocytes and a continuous cell line, Biochem. Biophys. Res. Commun. 333 (2005) 609–621.
[25] Y.Y. Choi, B.G. Chung, D.H. Lee, A. Khademhosseini, J.H. Kim, S.H. Lee, Controlled-size embryoid body formation in concave microwell arrays, Biomaterials 31 (2010) 4296–4303.
[26] F. Barry, R.E. Boynton, B. Liu, J.M. Murphy, Chondrogenic differentiation of mesenchymal stem cells from bone marrow: differentiation-dependent gene expression of matrix components, Exp. Cell Res. 268 (2001) 189–200.
[27] A.R. Poole, T. Kojima, T. Yasuda, F. Mwale, M. Kobayashi, S. Laverty, Composition and structure of articular cartilage: a template for tissue repair, Clin. Orthop. Relat. Res. (2001) S26–S33.
[28] C. Kiani, L. Chen, Y.J. Wu, A.J. Yee, B.B. Yang, Structure and function of aggrecan, Cell Res. 12 (2002) 19–32.
[29] AG cd, Efficacy and Safety Study of co.Don Chondrosphere to Treat Cartilage Defects, ClinicalTrials.gov, 2015.
[30] M.B. Mueller, M. Fischer, J. Zellner, A. Berner, T. Dienstknecht, R. Kujat, et al., Effect of parathyroid hormone-related protein in an in vitro hypertrophy model for mesenchymal stem cell chondrogenesis, Int. Orthop. 37 (2013) 945–951.
[31] W. Zhang, J. Chen, S. Zhang, H.W. Ouyang, Inhibitory function of parathyroid hormone-related protein on chondrocyte hypertrophy: the implication for articular cartilage repair, Arthritis Res. Ther. 14 (2012) 221.